AlGaN/GaN Hetero-Junction Bipolar Transistor with Selective-Area Regrown n-type AlGaN Emitter

Lian Zhang[1], Jianping Zeng[2], Zhe Cheng[1], Hongxi Lu[1], Hongrui Lv[1,3] and Yun Zhang[1,3]*

[1]Institute of Semiconductors, Chinese Academy of Sciences, P.O. Box 912, Beijing 100083, China
[2]Microsystem and Terahertz Research Center, China Academy of Engineering Physics, Chengdu, 610299, China
[3]University of Chinese Academy of Sciences, Beijing 100049, China
Email: yzhang34@semi.ac.cn

Keywords: AlGaN/GaN, Hetero-junction bipolar transistor, MOCVD, regrowth

Abstract

We report on AlGaN/GaN hetero-junction bipolar transistors (HBTs) on sapphire substrates with metal-organic chemical vapor deposition (MOCVD) selective-area regrown n type AlGaN emitters. The metal-semiconductor contact on the p-GaN base layer is remarkably improved by using a dry-etching-free process. The HBT exhibits current density J_C of 4 kA/cm^2 and power density of ~ 60 kW/cm^2 observed from common-emitter I-V curves. These values are the highest reported for regrown GaN based HBTs. The open-base breakdown voltage (BV_{CEO}) is higher than 145 V which is comparable to direct-growth GaN-based HBTs. The maximum current gain h_{fe} calculated from the Gummel plot is around 6.

INTRODUCTION

GaN-based transistors combine advantages of high power handling capability, high voltage, and high temperature operation. Compared to high electron mobility transistors (HEMTs), heterojunction bipolar transistors (HBTs) have inherent advantages such as acceptable linearity, high current and power densities, and normally-off operation. Recently, GaN-based HBTs have shown high current gain (β) and high current and power densities [1]– [4]. A cut-off frequency (f_T) greater than 8 GHz was also demonstrated [5]. However, the maximum oscillation frequency (f_{max}) was no higher than 1.8 GHz even though InGaN was employed as the base material for relatively higher free hole concentration [5], [6]. Besides the low concentration and mobility of holes, another obstacle limiting f_{max} is dry-etching-induced damage to the base layer. Dry etching creates nitrogen vacancies on the surface of the p-type GaN or InGaN base layer, resulting in a Schottky metal-semiconductor contact [7]. Although wet repairing [8] and N_2-incorporated dry etching [9] were reported to remove the etching damage, the Schottky barrier still existed, resulting in high base-emitter junction voltage, which caused high power consumption. A regrown p-type InGaN or GaN external base contact layer [10]– [12] also has been used to address the etching damage issue, but it still needs accurate etching depth control on the emitter/base interface. On the other hand, regrown n-type emitter layers can avoid the etching process [13]– [15]. An AlGaN/GaN HBT with a selective-area regrown emitter was reported to reach a high operation voltage of > 300 V [14]. In Ref. [15], ammonia molecular beam epitaxy (NH_3 MBE) was used to grow AlGaN/GaN HBTs with regrown external base contact layers and emitter layers for reducing the leakage current induced by dislocations.

In this work, we demonstrate AlGaN/GaN HBTs with selective-area regrown n-type AlGaN emitters by metal-organic chemical vapor deposition (MOCVD). Improved contact on the p-GaN base layer is achieved by avoiding dry etching. The current and power densities of the HBT are 4 kA/cm^2 and 60 kW/cm^2 in common-emitter operation. These high values benefit from high base conductivity, which allows higher base current. The open-base breakdown voltage (BV_{CEO}) reaches 145 V, which is comparable to reported direct-growth GaN-based HBTs. Due to high recombination currents, the maximum h_{fe} in the Gummel plot is only slightly over 6. The β may be greatly improved through optimizing the base thickness, device layout design, and regrown interface.

WAFER GROWTH AND DEVICE FABRICATION

The AlGaN/GaN HBT was grown by MOCVD. Trimethyl gallium (TMGa) and trimethyl aluminum (TMAl) were used as alkyl sources, and ammonia (NH_3) was used as the hydride source. Silane (SiH_4) and bis(cyclopentadienyl)-magnesium (Cp_2Mg) were employed as n-type and p-type dopants. The layer structure growth started with a 2-μm unintentionally-doped (UID) GaN buffer layer on a sapphire substrate, followed by a 1-μm highly-doped n^+-GaN sub-collector, a 500-nm UID GaN collector layer, and a 100-nm p-type GaN base layer. Then, the wafer was taken out of the reaction chamber to prepare for the selective-area growth of the n-type AlGaN emitter. A SiO_2 mask layer was deposited on the wafer by plasma-enhanced chemical vapor deposition and patterned by photolithography and buffered oxide etch (BOE) wet etching to define the emitter area. Then the wafer with SiO_2 mask layer was taken back into the reaction

chamber of MOCVD and 100-nm of n-type AlGaN was regrown at 980 ℃ and 200 Torr in an H_2 ambient. The Al composition of the regrown n-type AlGaN emitter was determined by X-ray diffraction (XRD). For testing the electron concentration and mobility by Hall measurement, a planar n-type AlGaN layer is grown on an UID GaN template on a sapphire substrate in the same run with the regrown n-type AlGaN emitter layer.

After removing the SiO_2 mask by buffered oxide etch (BOE), the base-collector mesa was formed by inductively-coupled plasma (ICP) etching. Then Ni/Ag/Pt metal stacks were deposited and annealed as metal-semiconductor base contacts. Ti/Al/Ti/Au metal stacks were deposited as emitter and collector contacts. The critical distances between our contact metals and mesas, W_{EB} and W_{BC}, were both 5 μm. Transmission Line Method (TLM) tests were carried out to determine the sheet resistances (R_s) and the specific contact resistivities (ρ_c) of the base, emitter, and collector. DC characteristics of the AlGaN/GaN HBT device were tested using an Agilent B1500A analyzer at the room temperature.

RESULTS AND DISCUSSION

The hole concentration of the p-type GaN base layer is 9.8×10^{17} /cm^3 with a mobility of 14.1 cm^2/V•s. The electron concentration and mobility of the regrown n-type AlGaN emitter layer are 7.4×10^{18} /cm^3 and 245 cm^2/ V•s. A regrown n-type AlGaN region with area of 5×7 mm^2 designed for XRD testing on the same HBT wafer shows that the Al component is ~7.9%.

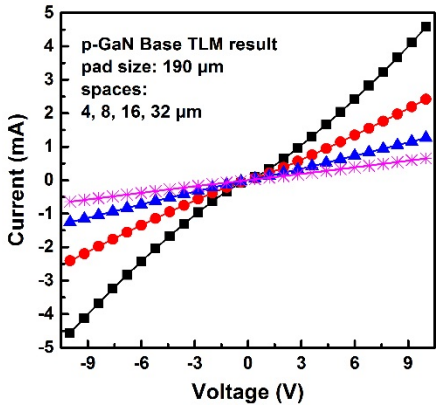

Fig. 1. TLM results of the p-GaN base layer.

I-V curves of TLM contact pads on the 100-nm-thick p-type GaN base layer are plotted in Figure 1. Ohmic contact is achieved although the I-V curves of the pads with a 4-μm space is not perfectly linear. For direct-growth HBTs, the contact on a dry-etched p-type InGaN base layer with the hole concentration of 2×10^{18}/cm^3 is obviously a Schottky barrier [7]. We attribute the good p-type base contact characteristics to the elimination of p-GaN base dry-etching process by using the selective-area emitter regrowth method.

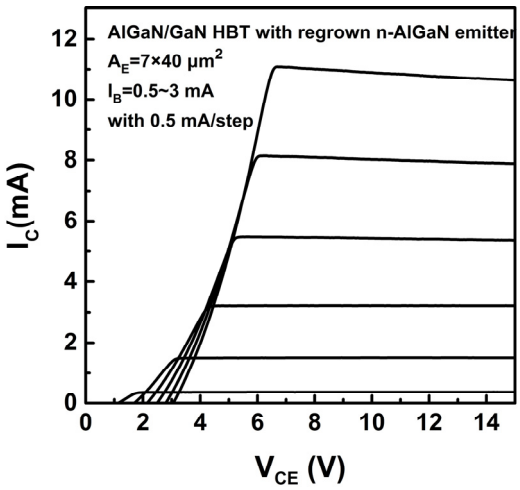

Fig. 2. Common-emitter family curves of the AlGaN/GaN HBTs.

Common-emitter family curves of the HBT with emitter area (A_E) = 7×40 μm^2 were characterized with V_{CE} from 0 to 15 V and the base current from 0.5 mA to 3 mA, 0.5 mA per step, as shown in Figure 2. The collector current density J_C is up to 4 kA/cm^2 at V_{CE}=11 V. A DC power density of ~ 60 kW/cm^2 is also attained at V_{CE}= 15 V. These values are the highest reported values on regrowth GaN-based HBTs. The high J_C and power density benefit from the realization of base ohmic contact, which increases the base conductivity, and consequently enhances the base current injection.

We also notice that the offset voltage (V_{offset}) is from 1.2 V to 3 V in Figure 2. The V_{offset} results from a combination of the different turn-on voltages for the base-emitter junction and collector-base junction, different junction areas, and resistive voltage drops between the external base contact and intrinsic device [16]. On the other hand, knee voltage (V_{knee}) less than 6 V also can be observed in the common-emitter family curves. The V_{knee} is among the lowest values reported for regrown GaN-based HBTs, thanks to the relatively low spreading resistance [17]. Both V_{offset} and V_{knee} can be further reduced by down scaling the device layout.

Gummel plot curves were measured at V_{BC} = 0 V, as shown in Figure 3. I_B and I_C cross over at 900 μA and V_{BE} = 6.3 V. The high crossover current indicates that the base generation-recombination current (I_{Br}) is high [18]. The current gain β (= I_C/I_B) reaches its maximum value over 5 at V_{BE} = 12 V with I_B = 10 mA and I_C = 50 mA. The relatively low β may be because of high I_{Br}. The h_{fe} (= dI_C/dI_B) is also given in Figure 3 and reaches a maximum value of 6 at V_{BE} = 11.5V. The fact of h_{fe} being higher than β may be due to trap states at the base-emitter junction, including surface states and interface states [18].

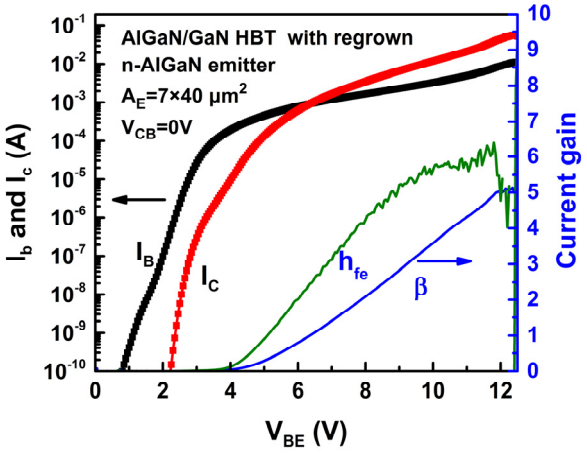

Fig. 3. Gummel plot curves of the AlGaN/GaN HBT.

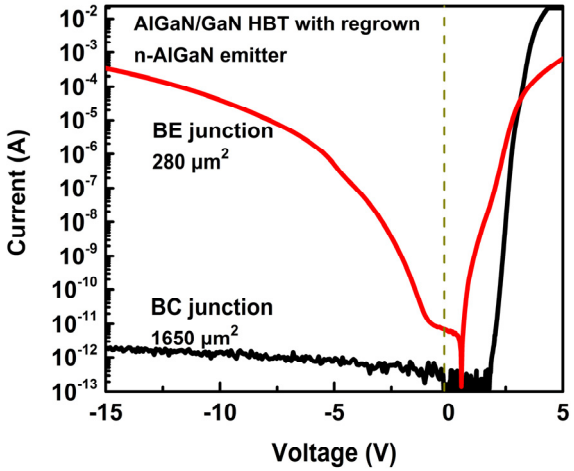

Fig. 4. The I-V characteristics of the base-collector junction and base-emitter junction of the AlGaN/GaN HBT.

An open-base breakdown voltage (BV_{CEO}) of 145 V on the AlGaN/GaN HBT with a 500-nm UID GaN collector is achieved. Because the emitter, base, and sub-collector all have much higher carrier concentrations than the UID GaN collector layer, the voltage mainly falls on the UID GaN collector layer, and the field is considered approximately uniform. Therefore, the breakdown field is ~2.9 MV/cm, which is comparable to reported direct-growth GaN based HBTs [1], and much higher than that of reported regrown GaN based HBTs. This result proves the great advantage of high voltage for GaN-based HBTs grown by MOCVD.

To further analyze the high base recombination current, the I-V curves of the base-emitter junction and base-collector junction on the same HBT were measured from -15 V to 5 V, as shown in Figure 4. The base-collector junction shows good current rectification characteristics. The turn-on voltage is about 2 V, and the leakage current is around 2 pA at -15 V. Before the base-collector junction turns on, the generation-recombination current in the depletion region is lower than 1 pA. These results reveal that the base-collector junction has good crystal quality. That is why the HBT has high BV_{CEO}. However, on the other hand, the base-emitter junction suffers much higher reverse leakage current and generation-recombination current, despite its smaller mesa area than the base-collector junction. The source of this may be the defects on the regrown interface between the p-GaN base and n-AlGaN emitter. Furthermore, these defects can act as carrier traps and dramatically increase base recombination currents, resulting in low current gain. Other reasons that the current gain may be lower include Al/Si diffusion during AlGaN emitter growth [19], the triangular quantum well formed near the abrupt base-emitter junction interface, the relatively thick base layer, and the large external base design.

CONCLUSIONS

We demonstrated n-p-n structure AlGaN/GaN HBTs with selective-area regrown n-type AlGaN emitters by MOCVD. Compared with other reported HBTs with base-emitter mesa dry-etching processes, the p-type base metal-semiconductor contact shows ohmic contact behavior owing to dry-etch-free processing. As a result, a high J_C of 4 kA/cm² and power density of ~ 60 kW/cm² are obtained on the HBT. The open-base breakdown voltage is 145 V, and as a consequence the breakdown field is ~2.9 MV/cm. These values are advanced compared to reported regrown GaN-based HBTs. The maximum β of the device is about 5 due to high base generation-recombination current I_{Br}.

ACKNOWLEDGEMENTS

The research is support in part by science challenge Project TZ2018003-2, national key R&D program of China under No.2017YFB0402900, and in part by the national natural science foundation of China under Grants Numbers. 61674143, 61376090, and 61474102.

REFERENCES

[1] S.-C. Shen, R. D. Dupuis, Z. Lochner, Y.-C. Lee, et al., Semi- cond. Sci. Technol. 28(7), 074025 (2013).
[2] Z. Lochner, H. J. Kim, S. Choi, Y.-C. Lee, et al., J. Cryst. Growth 315(1), 278-282 (2011).
[3] T. T. Kao, Y. C. Lee, H. J. Kim, J. H. Ryou, et al., Appl. Phys. Lett. 107(24), 242104 (2015).
[4] B. F. Chu-Kung, C. H. Wu, G. Walter, M. Feng, et al., Appl. Phys. Lett. 91(), 232114 (2007).
[5] R. Dupuis, H. J. Kim, Y.-C. Lee, Z. Lochner, et al., ECS Trans. 58(4), 261-267 (2013).
[6] S.-C. Shen, R. D. Dupuis, Y.-C. Lee, H.-J. Kim, et al., IEEE Electron Dev. Lett. 32(8), 1065-1067 (2011).

[7] C.-H. Wu, B. F. Chu-Kung and M. Feng, CS Mantech Conference, Chicago, Illinois, USA, May. 2008.
[8] Y.-C. Lee, Y. Zhang, H.-J. Kim, S. Choi, et al., IEEE Transactions on Electron Devices 57(11), 2964-2969 (2010).
[9] D. Kent, K. Lee, A. Zhang, B. Luo, et al., Solid-State Electron 45(3), 467-470 (2001).
[10] L. S. McCarthy, P. Kozody, M. Rodwell, S. DenBaars, et al., IEEE Electron Dev. Lett. 20(6), 277-279 (1999).
[11] B. S. Shelton, D. J. H. Lambert, J. J. Huang, M. M. Wong, et al., IEEE Trans. Electron Dev. 48(3), 490-494 (2001).
[12] T. Makimoto, K. Kumakura and N. Kobayashi, Jpn. J. Appl. Phys. 43(4B) (2004).
[13] K. P. Lee, A. P. Zhang, G. Dang, F. Ren, et al., Solid-State Electron. 45, 2443-247 (2001).
[14] H. Xing, P. M. Chavarkar, S. Keller, S. P. DenBaars, et al., IEEE Electron Dev. Lett. 24(3), 141-143 (2003).
[15] A. Raman, C. A. Hurni, J. S. Speck, and U. K. Mishra, Phys. Status Solidi A 209(1), 216-220 (2012).
[16] F. Ali and A. Gupta, *HEMTs & HBTs: Devices, Fabrication, and Circuits*, first ed., Artech House, Inc. Norwood, ch. 5, sec. 5.4, pp. 282-283 (1991).
[17] W. Liu, *Fundamentals of III-V Devices: HBTs, MESFETs, and HFETs/HEMTs*, first ed., New York, USA, a Wiley-Interscience publication, ch. 4, sec. 4-4, pp. 250-260 (1999).
[18] S.-C. Shen, Y.-C. Lee, H.-J. Kim, Y. Zhang, et al., IEEE Electron Dev. Lett. Vol. 30, no. 11, pp. 1119 (2009).
[19] Y. T. Tseng, C. W. Lin, W. C. Yang, K. Y. Chen, et al., IEEE Trans. Electron Dev., vol. 63, no. 11, pp. 4262-4266 (2016).

ACRONYMS

HBT: Heterojunction Bipolar Transistor
MOCVD: metal-organic chemical vapor deposition
NH_3 MBE: ammonia molecular beam epitaxy
HEMT: high electron mobility transistor
XRD: X-ray diffraction
ICP: inductively-coupled plasma
TLM: Transmission Line Method
BOE: buffered oxide etch
R_s: sheet resistance
ρ_c: specific contact resistivity
BV_{CEO}: open-base breakdown voltage
I_{Br}: base recombination current